Available online at www.sciencedirect.com
SCIENCE DIRECT®
Bioelectrochemistry 61 (2003) 29–38
Bioelectrochemistry
www.elsevier.com/locate/bioelechem

Electrochemical and electrocatalytic properties of myoglobin and hemoglobin incorporated in carboxymethyl cellulose films

He Huang, Pingli He, Naifei Hu*, Yonghuai Zeng

Department of Chemistry, Beijing Normal University, 19 Xinjiekouwai Street, Beijing 100875, PR China

Received 11 March 2003; received in revised form 26 May 2003; accepted 4 June 2003

Abstract

Protein-CMC films were made by casting a solution of myoglobin (Mb) or hemoglobin (Hb) and carboxymethyl cellulose (CMC) on pyrolytic graphite electrodes. In pH 7.0 buffers, Mb and Hb incorporated in CMC films gave a pair of well-defined and quasi-reversible cyclic voltammetric peaks at about −0.34 V vs. SCE, respectively, characteristic of heme Fe^{III}/Fe^{II} redox couples of the proteins. The electrochemical parameters such as apparent standard heterogeneous electron transfer rate constants (k_s) and formal potentials ($E^{\circ\prime}$) were estimated by square wave voltammetry with nonlinear regression analysis. In aqueous solution, stable CMC films absorbed large amounts of water and formed hydrogel. Scanning electron microscopy of the films showed that interaction between Mb or Hb and CMC would make the morphology of dry protein-CMC films different from the CMC films alone. Positions of Soret absorbance band suggest that Mb and Hb in CMC films retain their secondary structure similar to the native states in the medium pH range. Trichloroacetic acid, nitrite, oxygen, and hydrogen peroxide were catalytically reduced at protein-CMC film electrodes.

Keywords: Myoglobin; Hemoglobin; Carboxymethyl cellulose; Direct electrochemistry; Electrochemical catalysis

1. Introduction

Heme proteins are important proteins in living systems which contain at least one porphyrin complex of Fe or heme as the prosthetic group, and perform different physiological functions [1,2]. Myoglobin (Mb) is a single-chain heme protein with molecule weight of about 17,800. The polypeptide chain folds into several segments that serves to stabilize the conformation of iron heme through hydrophobic interaction and hydrogen bonding. Hemoglobin (Hb), with its molecule weight of about 66,000, is much larger than Mb. It contains four subunits, each of which is similar to Mb and contains one heme prosthetic groups [3]. In vertebrate animals, Mb and Hb functions in storing and transporting oxygen in muscle and blood, respectively [4]. As their structures, properties, and functions are now more clearly known than other globular proteins, and they are commercially available and relatively inexpensive, Mb and Hb are often used as an instructive model for studying the property and function of heme proteins or enzymes.

Direct electrochemistry of heme proteins arouses increasing interest in recent years [5,6]. With direct electrochemical reactions of proteins at electrodes, we are able to establish a model for studying the mechanism of electron transfer between enzymes in biological system and obtain information on their intrinsic properties of thermodynamics and kinetics. A marriage between electrodes and proteins that bear highly specific modes of catalytic or sensory action is highly desirable, and could become a foundation for fabricating the new generation of biosensors or bioreactors.

A relatively new approach to realize direct electrochemistry of proteins is to incorporate proteins into films that are modified on electrode surface [7,8]. Our long-term goal is to make stable protein films with good electroactivity and enzyme-like catalytic activity, which are amenable to various electrochemical, spectroscopic, and other experiments. Once useful films are developed using Mb or Hb, they can then be extended to other enzymes. Successful approaches in this respect have included cast films of proteins with insoluble surfactants [9,10], hydrogel polymers [11–14], polyelectrolyte-or clay-surfactant

* Corresponding author. Tel.: +86-10-6220-7838; fax: +86-10-6220-0567.
E-mail address: hunaifei@bnu.edu.cn (N. Hu).

1567-5394/$ - see front matter © 2003 Elsevier B.V. All rights reserved.
doi:10.1016/S1567-5394(03)00057-4

composites [15–18], clay nanoparticles [19], and films of proteins and polyions grown layer-by-layer [20–22]. All these films facilitate direct, reversible electron transfer between heme proteins and electrodes, and usually demonstrated good enzyme-like catalytic reactivity toward various substrates.

Cellulose is one of the naturally occurring biopolymers and widely present in the wood and other plants. Cellulose in its native form is not soluble in water. It can be rendered water-soluble by chemical reaction of its hydroxyl groups with hydrophilic substituents. Carboxymethyl cellulose (CMC) is one of the water-soluble cellulose derivatives. CMC contains a hydrophobic polysaccharide backbone and many hydrophilic carboxyl groups, and hence shows amphiphilic characteristic. Due to its desirable properties such as nontoxicity, biocompatibility, biodegradability, high hydrophilicity, and good film forming ability, CMC has been used in various practical fields [23]. CMC has also been used to study interactions with proteins. For example, Cark and Glatz described the formation of complex of CMC with casein by electrostatic interaction [24]. Lii et al. [25] reported the formation of CMC-casein complex by covalent bonds with electrosynthesis. These complexes were very stable to pH and ionic strength changes and exhibited very good emulsifying properties and increased thermal stability. We thus expect that CMC may provide a new and different matrix for immobilization of proteins, and CMC films may be used as a suitable microenvironment for redox proteins to exchange electron directly with underlying electrodes. To our best knowledge, direct electrochemistry of proteins or enzymes at CMC-modified electrodes has not been reported until now.

In this paper, two heme proteins including Mb and Hb were incorporated in CMC films modified on pyrolytic graphite (PG) electrodes. The direct electrochemistry of the proteins in CMC films was studied. The protein-CMC films were also characterized by UV–Vis spectroscopy and scanning electron microscopy. Electrocatalytic properties of protein-CMC films toward different substrates such as trichloroacetic acid, nitrite, oxygen, and hydrogen peroxide were also discussed.

2. Materials and methods

2.1. Materials

Horse heart myoglobin (Mb, MW 17,800) and human hemoglobin (Hb, MW 66,000) were from Sigma and used as received without further purification. Sodium carboxymethyl cellulose (CMC) was from Beijing Donghuan Associated Chemicals. Trichloroacetic acid (TCA) was from Beijing Dongjiao Chemical Engineering Plant. Sodium nitrite ($NaNO_2$) was from Beijing Shuanghuan Chemicals. Hydrogen peroxide (H_2O_2, 30%) was from Beijing Chemical Engineering Plant. All other chemicals were reagent grade.

Buffers were 0.1 M sodium acetate, 0.05 M sodium dihydrogen phosphate, 0.05 M boric acid, or 0.05 M citric acid, all containing 0.1 M KBr. Buffer pH was adjusted with HCl or NaOH solutions. Solutions were prepared using deionized water which was purified twice successively by ion exchange and distillation.

2.2. Preparation of modified electrodes

Prior to coating, basal plane pyrolytic graphite (PG, Advanced Ceramics, geometric area 0.16 cm^2) electrodes were polished by hand with metallographic sandpaper of 1200 grit while flushing with pure water. Electrodes were then ultrasonicated in pure water for 30 s.

A CMC solution (4 mg ml^{-1}) was prepared by dissolving CMC in water with ultrasonication for about 1 h. To obtain the best CV responses of protein-CMC films, the concentration of proteins, the volume ratio of protein/CMC, and the total volume of protein-CMC solution were optimized. Typically, 10 μl of solution containing 5.6×10^{-5} M Mb or 1.5×10^{-5} M Hb and 2 mg ml^{-1} CMC were spread evenly onto PG electrode surface. After being dried in air overnight, the protein-CMC films were formed on PG.

2.3. Apparatus and procedures

A CHI 660 electrochemical workstation (CH Instruments) was used for cyclic voltammetry (CV) and square wave voltammetry (SWV) as described previously [18]. A conventional three-electrode cell was used with a saturated calomel electrode (SCE) as reference. Voltammetry on electrodes modified with protein-CMC films was run in buffers containing no proteins. Buffers were purged with highly purified nitrogen for at least 20 min prior to a series of voltammetric experiments. A nitrogen environment was then kept in the cell by continuously bubbling N_2 during the whole experiment. In the experiment with oxygen, measured volumes of air were injected through solutions via a syringe in a cell that had been previously degassed with purified nitrogen. All experiments were done at ambient temperature (18 ± 2 °C).

UV–Vis spectroscopy was done with a Cintra 10 e UV–Vis spectrophotometer (GBC). Sample films for spectroscopy were prepared by depositing protein-CMC solutions onto glass slides with the same concentration as for PG electrodes as described above. Scanning electron microscopy (SEM) was done with an X-650 scanning electron microanalyzer (Hitachi) at an acceleration voltage of 20 kV. Sample films were prepared on PG disks with the same method as for voltammetry. The samples were fixed on the SEM mounting stage with conductive two-sided adhesive tapes. Prior to SEM analysis, the films were coated with Au by an IB-3 ion coater (Eiko).

3. Results and discussion

3.1. Voltammetry

When Mb-CMC and Hb-CMC film electrodes were placed in protein-free pH 7.0 buffers, after several CV scans, a pair of quasi-reversible reduction–oxidation peaks was observed with an average peak potential at about − 0.34 V vs. SCE for both protein-CMC films. The steady state of CV for Hb-CMC and Mb-CMC films was shown in Fig. 1b and Fig. 1c, respectively. The peaks were located at the potentials characteristic of heme Fe^{III}/Fe^{II} redox couples of the proteins [26,27]. No voltammetric signal was observed at plain CMC film electrodes in the same potential window (Fig. 1a). This indicates that CMC films would have a great effect on the kinetics of the electrode reaction for Mb and Hb, and provide a favorable microenvironment for the proteins to transfer electrons with underlying PG electrodes. While the exact nature of this effect is not yet very clear, the role of films in enhancing electron transfer is probably related to the formation of CMC hydrogel in solution, which is compatible with the biomolecules. Another possibility is that the CMC films may inhibit adsorption of the impurities or denatured proteins in Mb or Hb solutions, which would otherwise block electron transfer between the proteins and electrodes [28].

For Hb-CMC films, the peak current quickly reached the steady state after several CV cycles, while for Mb-CMC films, the peak currents increased with soaking time and reached the steady state in about 3 h. Thus, all following electrochemical experiments with protein-CMC films were done at their steady states. CVs of the two protein-CMC films had roughly symmetric peak shapes and nearly equal heights of reduction and oxidation peaks. The reduction peak currents were linearly proportional to scan rates from 0.05 to 2 V s^{-1}. Integration of reduction peaks gave nearly constant charge (Q) values with different scan rates. All these are characteristic of surface-confined or thin-layer electrochemical behavior [29]. On the forward cathodic scan, all electroactive Fe^{III} form of Mb or Hb in the films was converted to Fe^{II} form, while on the reverse anodic scan, the Fe^{II} form of the protein was completely transformed back to the Fe^{III} form. Using the integrals of the reduction peaks and Faraday's laws ($\Gamma^* = Q/(n\mathrm{FA})$) [29], the average surface concentration of electroactive proteins in CMC films (Γ^*) were estimated to be $(1.61 \pm 0.11) \times 10^{-11}$ mol cm^{-2} for Hb and $(1.51 \pm 0.03) \times 10^{-10}$ mol cm^{-2} for Mb. The fractions of electroactive proteins among total deposited proteins in CMC films were 1.7% for Hb and 3.6% for Mb. To explore the reason why the fraction of electroactive proteins in the films was so small, the influence of film thickness on the fraction was investigated. Taking Mb-CMC films as an example, various amounts of Mb-CMC solutions with the same Mb/CMC ratio were deposited on PG electrodes forming Mb-CMC films with different film thickness, and CVs were run to obtain the values of Q and Γ^*. Results showed that while the total surface concentration of electroactive Mb in the films (Γ^*) increased with the film thickness, the fraction of electroactive Mb decreased dramatically (Fig. 2), suggesting that only Mb in the inner layers of the films closest to the electrode surface can exchange electrons with the electrode. Similar behavior was also observed for other protein films [14,19].

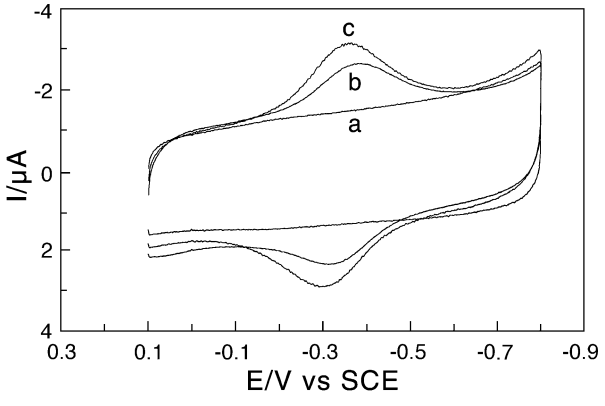

Fig. 1. Cyclic voltammograms at 0.2 V s^{-1} in pH 7.0 buffers for (a) CMC films, (b) Hb-CMC films, and (c) Mb-CMC films.

The CMC films could uptake proteins from their solutions. For instance, when protein-free CMC films on PG electrodes were placed into 0.03 mM Hb buffer solution at pH 7.0, the CV scans at different soaking times revealed the growth of the reversible CV peaks at about − 0.34 V. The peak currents showed no further increase in about 26 days, suggesting that the CMC films are fully loaded with Hb. When fully loaded Hb-CMC films were removed from the Hb solution, and transferred to a buffer containing no Hb at the same pH, their CV responses were identical to those in Hb solutions and quite stable. Both cast and immersing methods showed very similar peak positions and heights for protein-CMC films at the steady state, but the former was more convenient and quantitative, and thus used for preparing protein-CMC films for the following studies.

From the pK_a values of 4.2–4.4 for carboxylic groups of CMC [25], it could be predicted that in pH 7.0 solution, the CMC films would carry negative charges. Mb and Hb, with their isoelectric points at 6.8 [30] and pH 7.4 [31], respectively, are essentially neutral at pH 7.0. However, they have a considerable number of amine and imine side chains on their surfaces. Taking Mb as an example, among the total 153 amino-acid residues, there are 19 lysine, 2 arginine, and 11 histidine residues which have side chains containing amine or imine groups [4]. The pK_a values for lysine and arginine residues are in the range of 10–11 and 12–13, respectively, while histidine residues have pK_a values close to pH 7 [32–34]. Thus, at pH 7.0, all surface lysine and arginine residues of Mb are protonated and have positive charges, although the net charge of Mb is close to zero. Thus, it would be possible that the driving force for Mb in pH 7.0 buffers to enter CMC films is the electrostatic

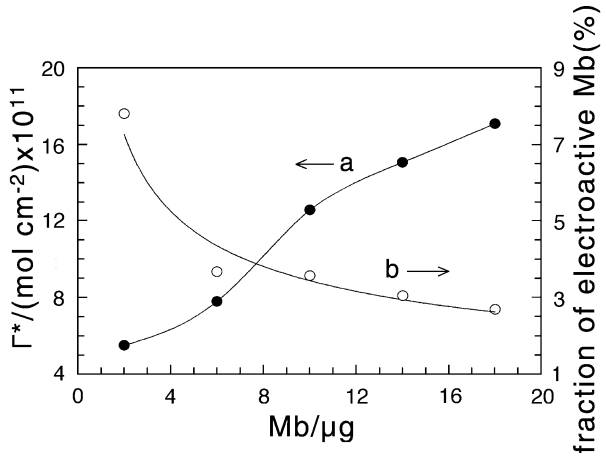

Fig. 2. Surface concentration of Mb (a) and fraction of electroactive Mb (b) for Mb-CMC films with different amounts of Mb with a constant ratio of Mb/CMC.

attraction between negatively charged carboxylic groups of CMC and positively charged lysine and arginine residues of Mb. This Coulombic interaction might also be responsible for the good stability of Mb-CMC films in the solution phase. Hb contains four subunits, each of which has component and structure very similar to Mb, and thus has the surface charge situation similar to Mb. Theoretically, the charge transport involving Mb and Hb within CMC films is dependent on both physical diffusion of the proteins and electron self-exchange between the protein molecules. Considering the slow diffusion of Mb and Hb within CMC films, the electron self-exchange or "electron hopping" may mainly contributes to the charge transport for the protein-CMC films.

The stability of protein-CMC films was tested by CV with both "wet" and "dry" methods. In the former case, a PG electrode coated with protein-CMC films was always stored in pH 7.0 buffers, and CVs were run periodically. Alternatively, a protein-CMC film electrode was stored in air for most of the storage time, and CVs were run periodically after returning the dry electrode to buffer solutions. With both methods, the protein-CMC films showed excellent stability. The CV peak potentials and currents were essentially unchanged for at least 30 days.

Square wave voltammetry [35] was used to obtain the electrochemical parameters with nonlinear regression analysis. The regression model for SWV forward and reverse curves was a combination of the single-species thin-layer SWV model [36] and the E°′ dispersion model, as described in detail previously [37,38]. The analysis of SWV data for protein-CMC films showed accuracy of fits on the 5-E°' dispersion model over a range of amplitudes and frequencies. The average values of apparent standard heterogeneous electron transfer rate constant (k_s) and formal potential (E°′) obtained from fitting SWV data at pH 7.0 for the two protein-CMC films were estimated and listed in Table 1. The k_s values were 85 and 86 s^{-1} for Hb-CMC and Mb-CMC films, respectively. E°′ values estimated as a midpoint of CV reduction and oxidation peak potentials for the films are also listed, which are in good agreement with those obtained by SWV. The E°′ values determined by CV and SWV for protein-CMC films are closer than those in other protein films (Table 1). The reason for this is not clear yet. It probably has something to do with different film component.

The k_s values for Hb-CMC and Mb-CMC films may be larger or smaller compared with those of other corresponding protein films, but all of them are in the same order of magnitude relatively large (Table 1), indicating enhanced electron transfer rate of the proteins in a suitable film environment. The E°′ value of heme Fe^{III}/Fe^{II} couple for Hb is slightly more negative than that for Mb in CMC films. This trend is also true for protein-chitosan and protein-clay films, but opposite for protein-AQ films (Table 1). The E°′ value for one protein in CMC films is different from that for the same protein in other films [8]. For example, for Mb in didodecyldimethylammonium bromide (DDAB) films, the formal potential of Mb Fe^{III}/Fe^{II} couple was reported by Rusling et al. to be +0.013 V vs. NHE (−0.228 V vs. SCE) at pH 7.0 [37], about 0.10 V more positive than that for Mb-CMC films. This confirms a specific influence of the film environment on E°′ for heme proteins, as reported previously [37]. Film components may change potentials via interactions with the protein or by their influence on the electrode double layer.

3.2. Influence of pH

The shape and position of the Soret absorption band of iron heme may provide information about possible denaturation of heme proteins. Indeed, the wavelength of Soret band may not be a diagnostic criteria for the conformational variation of the whole proteins, however, it is sensitive to the conformational change in the heme region [39,40]. UV–Vis spectroscopy was thus used here to

Table 1
Apparent standard heterogeneous electron transfer rate constants and formal potentials for heme protein films on PG electrodes in pH 7.0 buffers containing no proteins

Films[a]	k_s/s^{-1}	Average E°′/V (vs. SCE)		Reference
		CV	SWV	
Mb-CMC	86 ± 22	−0.327	−0.330	tw[b]
Hb-CMC	85 ± 25	−0.349	−0.354	tw[b]
Mb-CS	82 ± 22	−0.330	−0.315	[14]
Hb-CS	104 ± 34	−0.337	−0.344	[14]
Mb-clay	50 ± 3	−0.342	−0.358	[18]
Hb-clay	31 ± 2	−0.347	−0.360	[18]
Mb-AQ	52 ± 6	−0.362	−0.340	[11]
Hb-AQ	62 ± 7	−0.341	−0.324	[12]

[a] CMC = carboxymethyl cellulose, CS = chitosan, AQ = Eastman AQ.
[b] tw: this work, reporting average values for analysis of eight SWVs at frequencies of 100–180 Hz, amplitudes of 60–75 mV, and a step height of 4 mV.

detect the change of Soret band of Mb and Hb in CMC films cast on the glass slides. Taking Hb-CMC films as an example, both dry films cast from Hb and Hb-CMC solutions showed Soret bands at 412 nm (Fig. 3a and b), suggesting that Hb in dry CMC films has a secondary structure nearly the same as the native state of Hb in its dry films alone. The dependence of the Soret band position on pH of external solution for Hb-CMC films was also tested. At pH 5.5 and 7.0, the Soret band appeared at 412 nm (Fig. 3d and e), same as for dry Hb-CMC films and dry Hb films alone, indicating that Hb essentially retains its native state at medium pH. Even at pH 3.5, the Soret band of the films still kept its position at 412 nm while the peak became smaller (Fig. 3c). At pH 10.0, however, the Soret band showed peak shape distortion, and was even hardly observed (Fig. 3f), suggesting that Hb in Hb-CMC films denatures to a considerable extent in this more basic environment. Although Hb-CMC films on glass slides were not as stable as on PG electrodes, they were stable enough to undergo the spectroscopic experiments in buffers. Mb-CMC films demonstrated the spectroscopic behavior very similar to Hb-CMC films.

CVs of protein-CMC films showed great dependence on pH of external buffers. An increase in buffer pH caused a negative shift in both reduction and oxidation peaks. The formal potentials ($E^{\circ\prime}$) of the heme Fe^{III}/Fe^{II} redox couple for the films, estimated as the average of CV reduction and oxidation peak potentials, showed a linear relationship with pH in the range of pH 2.5–12 with a slope of -45 mV pH^{-1} for Hb-CMC films and -41 mV pH^{-1} for Mb-CMC

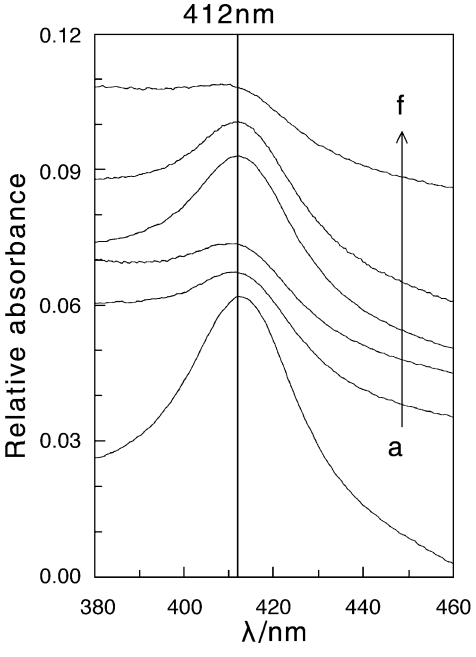

Fig. 3. UV–Vis spectra of (a) dry Hb films, (b) dry Hb-CMC films, and Hb-CMC films in different pH buffers: (c) pH 3.5; (d) pH 5.5; (e) pH 7.0; (f) pH 10.0. The absorbance coordinate only reflects relative absorbance.

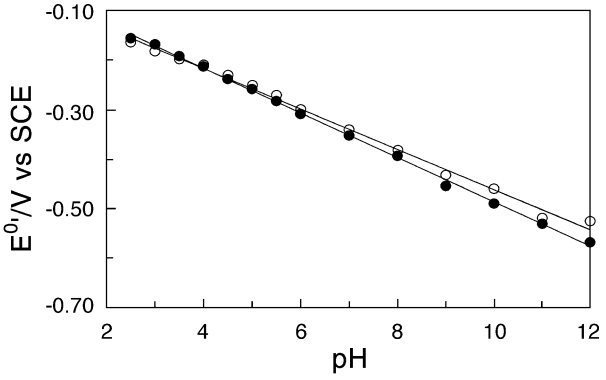

Fig. 4. Influence of pH on formal potentials for (○) Mb-CMC films and (●) Hb-CMC films from CV at 0.2 V s^{-1}.

films (Fig. 4). These slopes are smaller than the theoretical value of -57.6 mV pH^{-1} at 18 °C for a reversible one-proton coupled single-electron transfer during electrochemical reduction [41,42]. While the reason for this is not clear yet, the linear correlation between $E^{\circ\prime}$ and pH at least suggests that the electron transfer between Mb or Hb in CMC films and PG electrodes is accompanied by proton transportation. The changes in CV peaks with pH were reversible for protein-CMC films. For example, CVs for Hb-CMC films at pH 7.0 were reproduced after immersing of the films in pH 5.5 buffers and then returning the films to the pH 7.0 buffers.

Mb and Hb in CMC films essentially retained their native state in the medium pH range of about 4–9. Beyond this pH range, at least a partial denaturation of Mb and Hb was detected by the UV–Vis spectra, while the well-defined and quasi-reversible CVs for protein-CMC films could still be observed. This suggests that CMC films may provide a better microenvironment for Mb and Hb so that they can keep their electrochemical activity in the relatively acidic or basic solution.

3.3. Effect of water

The effect of water on CMC and protein-CMC films was investigated, and the weighing method was used to estimate the water content of the films. For example, thick CMC and Hb-CMC films were cast on glass slides and dried completely in air. The clear and transparent dry films were then soaked in water for 1 h so that the films were fully swelled and saturated by water. At the fully swelled state, both CMC and Hb-CMC films demonstrated the volume about 10 times larger than the original dry one, and took on an opaque appearance. The weighing results before and after saturated hydration showed that water accounted for about 97% and 95% for CMC and Hb-CMC films, respectively. CMC films with such a high content of water formed hydrogel. Thus, the environment in which Mb or Hb resides is mainly aqueous. This may explain why the Soret band spectra of protein-CMC films are the same as those of the proteins in

water at the same pH. The more loosening structure of CMC in its hydrogel form may also provide a more suitable microenvironment for Mb or Hb to transfer electrons with underlying PG electrodes.

3.4. Morphology of the films

The morphology of dry CMC and protein-CMC films measured by SEM were compared (Fig. 5). Top views of a CMC film on a PG disk demonstrated a wide leaf-like structure without formation of crystal (Fig. 5a). However, with the same magnification, the SEM top views of protein-CMC films showed different morphology. Both Hb-CMC and Mb-CMC films demonstrated a cypress leaf-like crystal structure in some area in their SEM pictures (Fig. 5b and c), but in the former the forming of crystal structure was more significant. CMC may interact with Mb or Hb and influence the morphology of the dry films. This interaction may also be responsible for the retention of the proteins in CMC films. CMC and protein-CMC films on very thin PG disks were freeze-fractured in liquid nitrogen, and the thickness of the films was estimated by SEM cross-section view to be about 2–5 μm.

3.5. Catalytic reactivity

Electrocatalytic behavior of Hb-CMC and Mb-CMC films was tested and characterized by CV with various substrates such as trichloroacetic acid (TCA), nitrite, oxygen, and hydrogen peroxide.

For electrocatalytic reduction of TCA, we took Mb-CMC film electrodes as an example. When TCA was added to a pH 3.0 buffer, an increase in the $MbFe^{III}$ reduction peak at about -0.2 V was observed, accompanied by a decrease of the $MbFe^{II}$ oxidation peak (Fig. 6a and b). The reduction peak current increased as the TCA concentration increased (Fig. 6c). Compared with the direct reduction of TCA on Mb-free CMC films at the potential more negative than -1.1 V, Mb-CMC films lowered the reduction overpotential of TCA by at least 0.9 V. The $MbFe^{III}$ in CMC films was electrochemically reduced at electrodes forming $MbFe^{II}$. The electrode reaction product $MbFe^{II}$ was then chemically oxidized by TCA and returned to $MbFe^{III}$. This formed a catalytic cycle, which presumably resulted in the reductive dechlorination of TCA [43]. The catalytic efficiency, expressed as the ratio of reduction peak current of $MbFe^{III}$ in the presence (I_c) and absence of TCA (I_d), I_c/I_d, decreased with increase of scan rate, also characteristic of electrochemical catalysis [44]. The catalytic reduction peak current showed a linear relationship with TCA concentration in the range of 7.5×10^{-4}–2×10^{-3} M, with a correlation coefficient of 0.998. Similar catalytic behavior toward TCA was also observed for Hb-CMC films.

Protein-CMC film electrodes were also used to electrochemically catalyze reduction of nitrite. For example, when an Mb-CMC film electrode was placed in a pH 5.5 buffer containing NO_2^-, a new reduction wave appeared at about -0.8 V while the original Mb Fe^{III}/Fe^{II} peak pair at about

Fig. 5. Top SEM views of coated PG electrodes with the same magnification of 500 for (a) CMC films, (b) Hb-CMC films, and (c) Mb-CMC films.

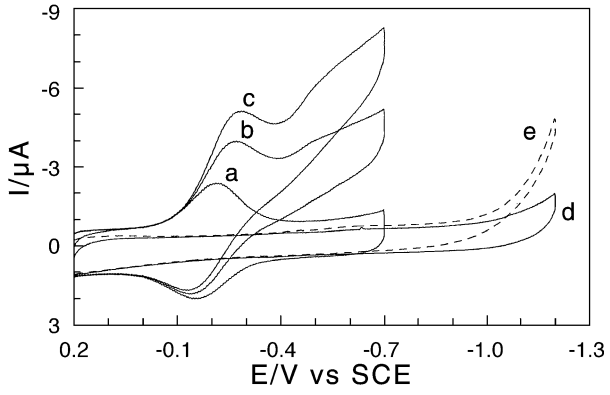

Fig. 6. Cyclic voltammograms at 0.08 V s^{-1} in pH 3.0 buffers for (a) Mb-CMC films in a buffer containing no TCA, (b) Mb-CMC films in a buffer containing 0.25 mM TCA, (c) Mb-CMC films in a buffer containing 0.5 mM TCA, (d) CMC films in a buffer containing no TCA, and (e) CMC films in a buffer containing 1.9 mM TCA.

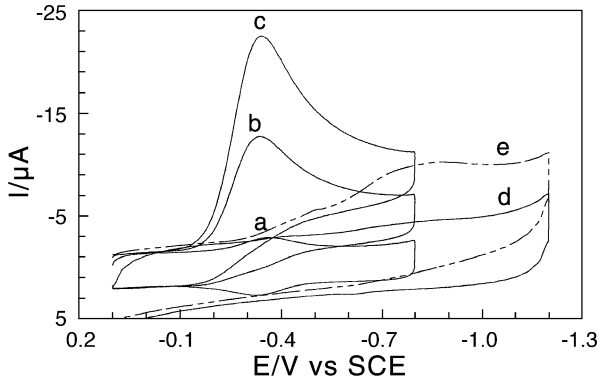

Fig. 8. Cyclic voltammograms at 0.2 V s^{-1} in 10 ml of pH 7.0 buffers for (a) Hb-CMC films with no oxygen present, (b) Hb-CMC films after 40 ml of air was injected into a sealed cell, (c) Hb-CMC films after 60 ml of air was injected, (d) CMC films with no oxygen present, (e) CMC films after 60 ml of air was injected.

−0.25 V was intact (Fig. 7a and b). This new wave increased with the concentration of NO_2^- (Fig. 7c). Direct reduction of NO_2^- at plain CMC film electrodes was observed at the potential more negative than −1.3 V (Fig. 7e). The overpotential required for the reduction of NO_2^- was thus lowered by Mb-CMC films by at least 0.5 V. The catalytic reduction wave of nitrite increased linearly with nitrite concentration in the range of 0.6–8 mM with a detection limit of 0.32 mM and a correlation coefficient of 0.999. Hb-CMC films showed very similar catalytic property toward nitrite. The mechanism of the catalytic reduction of NO_2^- at protein-CMC film electrodes is not clear yet. It is probably similar to that at Mb-DDAB film electrodes, in which N_2O was detected by mass spectroscopy on electrolysis at −0.895 V in pH 7.4 buffers [45].

The reduction of oxygen was electrocatalyzed by protein-CMC film electrodes. Take Hb-CMC films as a representative example. When a certain volume of air was passed through a pH 7.0 buffer by a syringe, compared to the reduction peak of the Hb-CMC films without oxygen present (Fig. 8a), a significant increase in reduction peak at about −0.4 V was observed, accompanied by the disappearance of the $HbFe^{II}$ oxidation peak (Fig. 8b). An increase in the amount of oxygen in solution increased the reduction peak current (Fig. 8c). Direct reduction of oxygen at CMC film electrodes occurred at about −0.8 V, about 0.4 V more negative than the potential of the catalytic peak. The catalytic efficiency (I_c/I_d) decreased with increase of scan rate. All these results are characteristic of reduction of oxygen by electrochemical catalysis with Hb-CMC films [44].

The electrocatalytic reduction of hydrogen peroxide by protein-CMC films was also tested by CV. For example, Fig. 9 showed the CV responses of Hb-CMC film electrodes in pH 7.0 buffers with and without H_2O_2 at the same scan rate. In the presence of H_2O_2, the

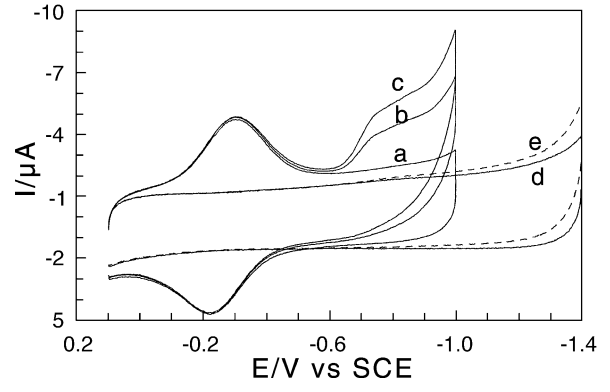

Fig. 7. Cyclic voltammograms at 0.2 V s^{-1} in pH 5.5 buffers for (a) Mb-CMC films in a buffer containing no $NaNO_2$, (b) Mb-CMC films in a buffer containing 3.6 mM $NaNO_2$, (c) Mb-CMC films in a buffer containing 5.6 mM $NaNO_2$, (d) CMC films in a buffer containing no $NaNO_2$, (e) CMC films in a buffer containing 5.6 mM $NaNO_2$.

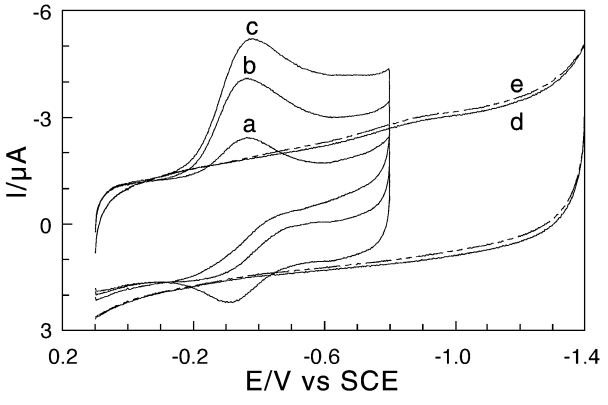

Fig. 9. Cyclic voltammograms at 0.2 V s^{-1} in pH 7.0 buffers for (a) Hb-CMC films in a buffer containing no H_2O_2, (b) Hb-CMC films in a buffer containing 0.044 mM H_2O_2, (c) Hb-CMC films in a buffer containing 0.084 mM H_2O_2, (d) CMC films in a buffer containing no H_2O_2, and (e) CMC films in a buffer containing 0.084 mM H_2O_2.

reduction peak at about −0.4 V increased dramatically and the oxidation peak almost disappeared. The reduction peak current increased with the concentration of H_2O_2 in solution. However, direct reduction peak was not observed at CMC film electrodes in the presence of H_2O_2 in this potential range. The catalytic reduction peak current had a linear relationship with H_2O_2 concentration in the range of 2–48 μM. The calibration curve tended to level off when the concentration of H_2O_2 became larger. When H_2O_2 concentration was larger than 0.12 mM, the catalytic peak current even decreased, suggesting a progressive enzyme inactivation in the presence of high concentration of substrate [46].

With Hb-CMC film electrodes, the catalytic reduction peak potential for H_2O_2 was almost the same as that for O_2 (Figs. 8 and 9), indicating the similarity of reaction mechanism between the two systems. This phenomenon was also observed in Mb-CMC and other protein films [47,48]. The reason for this and the exact mechanism of catalytic reduction of hydrogen peroxide at protein-CMC film electrodes is not very clear yet. We speculate that in the presence of hydrogen peroxide, the Hb-CMC film system behaves like a horseradish peroxidase (HRP)/H_2O_2 or catalase/H_2O_2 system where H_2O_2 acts either as an oxidant or as a reductant [49,50]. Compound I, the oxidation product of $HbFe^{III}$ by H_2O_2 may be reduced by H_2O_2 through a two-electron transfer pathway and produce native $HbFe^{III}$ again and O_2 [49,50]. It is the production of O_2 that may make the electrochemical catalytic behavior of H_2O_2 very similar to that of O_2 at Hb-CMC film electrodes.

To investigate the influence of film thickness on catalytic reduction of hydrogen peroxide, various amounts of Mb-CMC solution with the same Mb/CMC ratio were deposited on PG electrodes, and the formed Mb-CMC films with different thickness were tested by CV in pH 7.0 buffers containing H_2O_2 with the same concentration. The results showed that the thickness of protein-CMC films had great influence on the catalytic properties of hydrogen peroxide. An increase in film thickness increases the total amount of electroactive Mb (Fig. 2a), and thus increases the catalytic reduction peak current (Fig. 10a). However, the catalytic efficiency decreased dramatically with the increase of film thickness (Fig. 10b), probably because the fraction of electroactive Mb in the films decreased accordingly (Fig. 2b). Another possible factor is that the thicker films would limit the diffusion of substrate within the films.

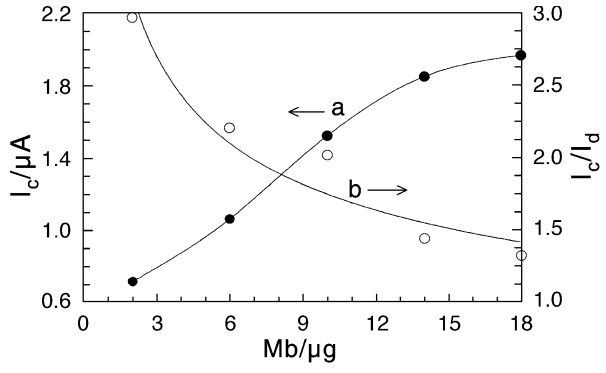

Fig. 10. Influence of amounts of Mb on (a) catalytic peak current (I_c) and (b) catalytic efficiency (I_c/I_d) for Mb-CMC films in pH 7.0 buffers, where I_d is the CV reduction peak current in buffers without H_2O_2 and I_c is the CV reduction peak current in buffers containing 0.044 mM H_2O_2.

Table 2
Catalytic efficiency or detection limit of different substrates with protein-CMC films

Films	Substrate			
	Catalytic efficiency (I_c/I_d)			Detection limit (mM)
	O_2[a]	H_2O_2[b]	TCA[c]	$NaNO_2$[d]
Mb-CMC	5.0	2.0	3.7	0.32
Hb-CMC	6.2	2.4	3.3	0.54

[a] 0.2 V s^{-1}, 20 ml air passed in 10 ml solution.
[b] 0.2 V s^{-1}, 0.044 mM H_2O_2.
[c] 0.08 V s^{-1}, 1.7 mM TCA.
[d] 0.2 V s^{-1}.

For comparison, the catalytic efficiencies for O_2, H_2O_2, and TCA with Hb-CMC and Mb-CMC film electrodes are listed in Table 2. The position of the new catalytic reduction peak of NO_2^- on protein-CMC films was very different from that of protein-CMC films in the absence of NO_2^- (Fig. 7). In this case, the catalytic efficiency cannot be defined. Thus, the values of detection limit are listed in Table 2 for the nitrite system. In general, Mb-CMC and Hb-CMC films demonstrate similar catalytic behavior toward all four substrates.

4. Conclusion

Biocompatible carboxymethyl cellulose can form stable films on pyrolytic graphite electrodes in aqueous solutions and provide a favorable microenvironment for Mb and Hb to transfer electron directly with underlying electrodes. Mb and Hb incorporated in CMC hydrogel films retained their native states. Good electrocatalytic properties of the protein-CMC films toward various substrates with biological or environmental significance, combined with excellent stability of the films, indicate that the protein-CMC films have a promising potential in fabricating the new generation biosensor or bioreactor based on the direct electrochemistry of proteins.

Acknowledgements

The authors thank the financial support from the National Natural Science Foundation of China (20275006, 29975003), and the State Key Laboratory of Electro-

analytical Chemistry of Changchun Institute of Applied Chemistry, the Chinese Academy of Sciences.

References

[1] T.E. Creighton, Proteins—Structure and Molecule Properties, Freeman, New York, 1984.
[2] A.I. Lehninger, D.L. Nelson, M.M. Cox, Principles of Biochemistry, 2nd ed., Worth, New York, 1993.
[3] M. Weissbluth, Molecular Biology: Biochemistry and Biophysics, vol. 15, Springer, New York, 1974.
[4] L. Stryer, Biochemistry, 3rd ed., Freeman, New York, 1988.
[5] F.A. Armstrong, H.A.O. Hill, N.J. Walton, Acc. Chem. Res. 21 (1988) 407.
[6] M.F. Chaplin, C. Bucke, Enzyme Technology, Cambridge University Press, Cambridge, UK, 1990.
[7] J.F. Rusling, Enzyme bioelectrochemistry in cast biomembrane-like films, Acc. Chem. Res. 31 (1998) 363–369.
[8] N. Hu, Direct electrochemistry of redox proteins or enzymes at various film electrodes and their possible applications in monitoring some pollutants, Pure Appl. Chem. 73 (2001) 1979–1991.
[9] J.F. Rusling, A.-E.F. Nassar, Enhanced electron transfer for myoglobin in surfactant films on electrodes, J. Am. Chem. Soc. 115 (1993) 11891–11897.
[10] J. Yang, N. Hu, Direct electron transfer for hemoglobin in biomembrane-like dimyristoyl phosphatidylcholine films on pyrolytic graphite electrodes, Bioelectrochem. Bioenerg. 48 (1999) 117–127.
[11] N. Hu, J.F. Rusling, Electrochemistry and catalysis with myoglobin in hydrated poly (ester sulfonic acid) ionomer films, Langmuir 13 (1997) 4119–4125.
[12] J. Yang, N. Hu, J.F. Rusling, Enhanced electron transfer for hemoglobin in poly (ester sulfonic acid) films on pyrolytic graphite electrodes, J. Electroanal. Chem. 463 (1999) 53–62.
[13] H. Sun, N. Hu, H. Ma, Direct electrochemistry of hemoglobin in polyacrylamide hydrogel films on pyrolytic graphite electrodes, Electroanalysis 12 (2000) 1064–1070.
[14] H. Huang, N. Hu, Y. Zeng, G. Zhou, Electrochemistry and electrocatalysis with heme proteins in chitosan biopolymer films, Anal. Biochem. 308 (2002) 141–151.
[15] H. Sun, H. Ma, N. Hu, Electroactive hemoglobin-surfactant-polymer biomembrane-like films, Bioelectrochem. Bioenerg. 49 (1999) 1–10.
[16] Y. Hu, N. Hu, Y. Zeng, Electrochemistry and electrocatalysis with myoglobin in biomembrane-like surfactant-polymer $2C_{12}N^{+}PA^{-}$ composite films, Talanta 50 (2000) 1183–1195.
[17] L. Wang, N. Hu, Electrochemistry and electrocatalysis with myoglobin in biomembrane-like DHP-PDDA polyelectrolyte-surfactant complex films, J. Colloid Interface Sci. 236 (2001) 166–172.
[18] X. Chen, N. Hu, Y. Zeng, J.F. Rusling, J. Yang, Ordered electrochemically-active films of hemoglobin, didodecyldimethylammonium ions and clay, Langmuir 15 (1999) 7022–7030.
[19] Y. Zhou, N. Hu, Y. Zeng, J.F. Rusling, Heme protein-clay films: direct electrochemistry and electrochemical catalysis, Langmuir 18 (2002) 211–219.
[20] Y. Lvov, Z. Lu, J.B. Schenkman, X. Zu, J.F. Rusling, Direct electrochemistry of myoglobin and cytochrome P450 in alternate layer-by-layer films with DNA and other polyions, J. Am. Chem. Soc. 120 (1998) 4073–4080.
[21] H. Ma, N. Hu, J.F. Rusling, Electroactive myoglobin films grown layer-by-layer with poly(styrenesulfonate) on pyrolytic graphite electrodes, Langmuir 16 (2000) 4969–4975.
[22] P. He, N. Hu, G. Zhou, Assembly of electroactive layer-by-layer films of hemoglobin and polycationic poly(diallyldimethyl ammonium), Biomacromolecules 3 (2002) 139–146.
[23] A.B. Savage, A.E. Young, A.T. Maasberg, Cellulose and cellulose derivatives, in: E. Ott, H.M. Sourlin, M.W. Grafflin (Eds.), High Polymers, vol. 5, Interscience, New York, 1954.
[24] K.M. Clark, C.E. Glatz, A binding model for the precipitation of proteins by carboxymethyl cellulose, Chem. Eng. Sci. 47 (1992) 215–224.
[25] H. Zaleska, P. Tomasik, C.-Y. Lii, Formation of carboxymethyl cellulose-casein complexes by electrosynthesis, Food Hydrocolloids 16 (2002) 215–224.
[26] Q. Huang, Z. Lu, J.F. Rusling, Composite films of surfactants, Nafion, and proteins with electrochemical and enzyme activity, Langmuir 12 (1996) 5472–5480.
[27] T. Ferri, A. Poscia, R. Santucci, Direct electrochemistry of membrane-entrapped horseradish peroxidase. Part I. A voltammetric and spectroscopic study, Bioelectrochem. Bioenerg. 44 (1998) 177–181.
[28] A.-E.F. Nassar, W.S. Willis, J.F. Rusling, Electron transfer from electrodes to myoglobin: facilitated in surfactant films and blocked by absorbed biomacromolecules, Anal. Chem. 67 (1995) 2386–2392.
[29] R.W. Murry, Chemically modified electrodes, in: A.J. Bard (Ed.), Electroanalytical Chemistry, vol. 13, Marcel Dekker, New York, 1986, pp. 191–386.
[30] A. Bellelli, G. Antonini, M. Brunori, B.A. Springer, S.G. Sligar, Transient spectroscopy of the reaction of cyanide with ferrous myoglobin— effect of distal side residues, J. Biol. Chem. 265 (1990) 18898–18901.
[31] J.B. Matthew, G.I.H. Hanania, F.R.N. Gurd, Electrostatic effects in hemoglobin–hydrogen-ion equilibria in human deoxyhemoglobin and oxyhemoglobin-A. 104, Biochemistry 18 (1979) 1919–1928.
[32] S.H. Friend, F.R.N. Gurd, Electrostatic stabilization in myoglobin. pH dependence of summed electrostatic contributions, Biochemistry 18 (1979) 4612–4619.
[33] D. Stigter, D.O.V. Alonso, K.A. Dill, Protein stability: electrostatics and compact denatured states, Proc. Natl. Acad. Sci. U. S. A. 88 (1991) 4176–4180.
[34] A.-S. Yang, B. Honig, Structural origins of pH and ionic strength effects on protein stability. Acid denaturation of sperm whale apomyoglobin, J. Mol. Biol. 237 (1994) 602–614.
[35] J.G. Osteryoung, J.J. O'Dea, Square-wave voltammetry, in: A.J. Bard (Ed.), Electroanalytical Chemistry, vol. 14, Marcel Dekker, New York, 1986, pp. 209–325.
[36] J.J. O'Dea, J.G. Osteryoung, Characterization of quasi-reversible surface processes by square-wave voltammetry, Anal. Chem. 65 (1993) 3090–3097.
[37] A.-E.F. Nassar, Z. Zhang, N. Hu, J.F. Rusling, T.F. Kumosinski, Proton-coupled electron transfer from electrodes to myoglobin in ordered biomembrane-like films, J. Phys. Chem. B 101 (1997) 2224–2231.
[38] Z. Zhang, J.F. Rusling, Electron transfer between myoglobin and electrodes in thin films of phosphatidylcholines and dihexadecylphosphate, Biophys. Chem. 63 (1997) 133–146.
[39] H. Theorell, A. Ehrenberg, Spectrophotometric, magnetic, and titrimetric studies on the heme-linked groups in myoglobin, Acta Chem. Scand. 5 (1951) 823–848.
[40] P. George, G. Hanania, Spectrophotometric study of ionizations in methemoglobin, Biochem. J. 55 (1953) 236–243.
[41] L. Meites, Polarographic Techniques, 2nd ed., Wiley, New York, 1965, pp. 282–284.
[42] A.M. Bond, Modern Polarographic Methods in Analytical Chemistry, Marcel Dekker, New York, 1980, pp. 29–30.
[43] A.-E.F. Nassar, J.M. Bobbitt, J.O. Stuart, J.F. Rusling, Catalytic reduction of organohalide pollutants by myoglobin in a biomembrane-like surfactant film, J. Am. Chem. Soc. 117 (1995) 10986–10993.
[44] C.P. Andrieux, C. Blocman, J.-M. Dumas-Bouchiant, F. M'Halla, J.M. Saveant, Homogeneous redox catalysis of electrochemical reactions; Part V. Cyclic voltammetry, J. Electroanal. Chem. 113 (1980) 19–40.
[45] R. Lin, M. Bayachou, J. Greaves, P.J. Farmer, Nitrite reduction by myoglobin in surfactant films, J. Am. Chem. Soc. 119 (1997) 12689–12690.

[46] S.A. Adediran, A.M. Lambeir, Kinetics of the reaction of Compound-II of horseradish-peroxidase with hydrogen-peroxide to form Compound-III, Eur. J. Biochem. 186 (1989) 571–576.
[47] R. Huang, N. Hu, Direct electrochemistry and electrocatalysis with horseradish peroxidase in Eastman AQ films, Bioelectrochemistry 54 (2001) 75–81.
[48] Z. Zhang, S. Chouchane, R.S. Magliozzo, J.F. Rusling, Direct voltammetry and catalysis with Mycobacterium tuberculosis catalase-peroxidase, peroxidases, and catalase in lipid films, Anal. Chem. 74 (2002) 163–170.
[49] R. Nakajima, I. Yamazaki, The mechanism of oxyperoxidase formation from ferryl peroxidase and hydrogen peroxide, J. Biol. Chem. 262 (1987) 2576–2581.
[50] M.B. Arnao, M. Acosta, J.A. del Rio, R. Varon, F. Garcia-Canovas, A kinetic study on the suicide inactivation of peroxidase by hydrogen peroxide, Biochim. Biophys. Acta 1041 (1990) 43–47.